

RESTRICTED

Copy No. 6
RM No. L9B25a

NACA RM No. L9B25a

~~UNCLASSIFIED~~

1115.5
~~NACA~~
64-112/6

c.1



RESEARCH MEMORANDUM

COMPARISON OF SEMISPAN DATA OBTAINED IN
THE LANGLEY TWO-DIMENSIONAL LOW-TURBULENCE PRESSURE
TUNNEL AND FULL-SPAN DATA OBTAINED IN THE
LANGLEY 19-FOOT PRESSURE TUNNEL FOR A WING
WITH 40° SWEEPBACK OF THE 0.27-CHORD LINE

By

FOR REFERENCE

Jones F. Cahill

Langley Aeronautical Laboratory
Langley Air Force Base, Va.

NOT TO BE TAKEN FROM THIS ROOM

CLASSIFICATION CANCELLED

Authority J.W. Crowley Date 12/14/53
FE 10501
By NACA 11/1/54
R.F. 1981

CLASSIFIED DOCUMENT

This document contains classified information affecting the National Defense of the United States within the meaning of the Espionage Act, USC 50:34 and 38. Its transmission or the revelation of its contents in any manner to an unauthorized person is prohibited by law. Information so classified may be imparted only to persons in the military and naval services of the United States, appropriate civilian officers and employees of the Federal Government who have a legitimate interest therein, and to United States citizens of known loyalty and discretion who of necessity must be informed thereof.

NATIONAL ADVISORY COMMITTEE FOR AERONAUTICS

WASHINGTON

April 22, 1949

UNCLASSIFIED

RESTRICTED



UNCLASSIFIED

NATIONAL ADVISORY COMMITTEE FOR AERONAUTICS

RESEARCH MEMORANDUM

COMPARISON OF SEMISPAN DATA OBTAINED IN
THE LANGLEY TWO-DIMENSIONAL LOW-TURBULENCE PRESSURE
TUNNEL AND FULL-SPAN DATA OBTAINED IN THE
LANGLEY 19-FOOT PRESSURE TUNNEL FOR A WING
WITH 40° SWEEPBACK OF THE 0.27-CHORD LINE

By Jones F. Cahill

SUMMARY

An investigation was made in the Langley two-dimensional low-turbulence pressure tunnel of a semispan model of a 40° sweptback wing of aspect ratio 4 and taper ratio 0.625, which had previously been tested in a full-span arrangement in the Langley 19-foot pressure tunnel, to obtain an indication of the validity of the semispan method of obtaining aerodynamic data in this particular arrangement. The results showed good agreement between the full-span and the semispan data at all Reynolds numbers for the plain wing, for the wing with semispan split flaps, for the wing with extensible leading-edge flaps, and at a high Reynolds number (6.8×10^6) for the wing with both leading-edge and split flaps deflected. At a low Reynolds number (3.0×10^6) with both flaps deflected, the lift and drag were also in good agreement, but the pitching-moment variation near maximum lift was unstable for the semispan tests whereas this variation was stable for the full-span tests.

This investigation indicates that data obtained from semispan wing tests may be expected to be in good agreement with data obtained from full-span tests of the wing alone except for unusually sensitive configurations, where the lift distribution is such that small disturbances produced by the tunnel-wall boundary layer may cause a radical change in the location of the original stall or in the manner in which the stall progresses.

Data obtained for the wing with both leading-edge and split flaps deflected show that the effect of leading-edge roughness is to cause the

~~RESTRICTED~~

UNCLASSIFIED

variation of pitching moments at the stall to change from stable to unstable. With roughness added, the full-span and semispan test results were in good agreement in all cases. Thus it appears that adding roughness minimizes the influence of the tunnel-wall boundary layer.

INTRODUCTION

The use of sweep to delay the effects of compressibility on the aerodynamic characteristics of aircraft wings has given rise to a need for data on wings of this type to aid designers in their evaluation of wing characteristics. Existing data have shown that the characteristics of swept wings may be subject to large and important scale effects (references 1 and 2). For this reason, it is desirable for tests to be run at Reynolds numbers as near as possible to those at which the wings are expected to be used.

In order to provide an additional facility for obtaining low-speed data on aircraft wings at Reynolds numbers approaching those encountered in flight, a semispan balance has recently been installed in the Langley two-dimensional low-turbulence pressure tunnel. This balance makes possible the testing of wing models at Reynolds numbers up to approximately 12×10^6 . The semispan arrangement was used in this installation because it permits tests of larger models (and therefore at higher Reynolds numbers) than a full-span arrangement. The semispan arrangement also leads to simpler model construction and elimination of external support interference.

Jet-boundary corrections have been derived for correcting data obtained from semispan tests to free-air conditions, but the question always exists as to whether the measured wing characteristics are affected by the presence of the tunnel-wall boundary layer. For this reason, tests were made of a model of a 40° sweptback wing which was geometrically similar to a model which had previously been tested in the Langley 19-foot pressure tunnel in a full-span arrangement. Tests were made of the plain wing, of the wing with a half-span split flap, and of the wing with a 0.725-span leading-edge flap. Effects of leading-edge roughness were determined for each of these configurations.

SYMBOLS

The data are presented in the form of standard NACA coefficients which are applicable to a full-span configuration.

C_L lift coefficient $\left(\frac{L}{qS}\right)$

C_D drag coefficient $\left(\frac{D}{qS}\right)$

C_m	pitching-moment coefficient $\left(\frac{M}{qS\bar{c}}\right)$
L	lift on semispan wing
D	drag on semispan wing
M	pitching moment of semispan wing about $\bar{c}/4$ (see fig. 1)
q	free-stream dynamic pressure $\left(\frac{\rho V^2}{2}\right)$
V	free-stream velocity
S	area of semispan wing
\bar{c}	mean aerodynamic chord $\left(\frac{1}{S} \int_0^{b/2} c^2 dy\right)$
α	angle of attack, degrees
R	Reynolds number
c	chord
y	distance along semispan
b	span of complete wing
ρ	mass density of air

APPARATUS AND TESTS

The balance from which the semispan model was supported is installed entirely outside the test section wall, and the wing is cantilevered through the tunnel wall and requires no supports in the air stream. The opening in the tunnel wall through which the model passes is closed by a labyrinth seal to minimize leakage at the model root without introducing undesirable friction forces. The portion of this seal which is exposed to the air stream is small so that the aerodynamic forces measured are, to a high degree of accuracy, only those on the model itself. A photograph of the model installed in the tunnel is shown in figure 2.

As discussed in reference 3, the Langley two-dimensional low-turbulence pressure tunnel is equipped with a blower which is used to control the boundary layer on the tunnel wall. Measurements of the wall boundary layer at the model location have shown that the boundary-layer total thickness at this point is approximately 1 inch for the operating conditions used in this investigation.

The model used in these tests is geometrically similar to the model used in tests in the Langley 19-foot pressure tunnel and described in reference 2. A sketch of the model is shown in figure 1. The wing sweep, defined as the sweep angle of the quarter-chord line of an equivalent straight wing, was 40° . This quarter-chord line becomes the 0.273-chord line of the swept wing, measured parallel to the plane of symmetry. The airfoil sections perpendicular to the 0.273-chord line are NACA 64₁-112. The wing had no geometric dihedral or twist and had an aspect ratio of 4 and a taper ratio of 0.625.

The split flaps used extended over the inboard 50 percent of the wing span, had a chord equal to 0.184 of the wing chord, and were deflected 60° in a plane perpendicular to the hinge line. Some tests were made with a solid wooden flap which formed a closed shape at the rear. Later tests made with a flap made of sheet metal showed discrepancies between drag measurements with the two types of flap. The open sheet-metal flap was, therefore, used for all further tests. The only data presented in this paper which were obtained with the solid flap are the data for the split-flap deflected condition with leading-edge roughness without the leading-edge flap. Details of the leading-edge flap are shown in figure 1(b). This flap is identical with the flap described in reference 4.

The model was made of aluminum alloy and was polished to a smooth finish. For the tests with leading-edge roughness, particles of carborundum having a diameter of approximately 0.008 inch were imbedded in thin shellac on both the upper and lower surfaces over a length of 0.08c from the leading edge. With the leading-edge flap installed, the roughness covered the flap as well as the portion of the wing surface normally roughened.

Tests were made at Reynolds numbers and Mach numbers which duplicated the conditions for the tests made of the full-span model in the Langley 19-foot pressure tunnel. Tests were made with the model in both the smooth and in the rough condition for the plain wing and for the wing with the trailing-edge split flap, with the leading-edge flap, and with both flaps together.

Jet-boundary corrections were applied to the data by the method described in reference 5. The values of the corrections to the angle of attack and drag coefficient were approximately

$$\Delta\alpha = 0.6C_L$$

$$\Delta C_D = 0.01C_L^2$$

RESULTS AND DISCUSSION

Comparisons between the semispan data obtained in this investigation and full-span data previously obtained in the Langley 19-foot pressure tunnel and presented in references 2, 4, 6, and 7 are shown in figures 3, 4, 5, and 6. The investigation of the various configurations of this wing in the Langley 19-foot pressure tunnel covered a long period of time and the results are presented in a number of papers. The data which were used for comparison with the data obtained in the Langley two-dimensional low-turbulence tunnel are those obtained when the model configuration was most nearly similar to the semispan model. For convenience in locating the original full-span data, the references and figure numbers in which the full-span data originally appeared are given in figures 3 to 6. In general, the agreement between the two sets of data is very good.

Slight differences are observed in maximum lift coefficients or in angles of attack for maximum lift in a few cases. Differences of this type occur frequently, however, when several tests are made of a given configuration in the same tunnel, particularly for wings in the range of thicknesses around 12 percent where conditions near maximum lift are rather critical. For this reason, no particular significance is attached to these differences.

The differences observed in drag coefficients are small in all cases except for the data for the model in the rough condition with the split flap deflected (fig. 5(b)). For this condition, the increase in drag coefficient measured for the semispan tests is attributed to the use of a split flap formed from a solid block. The drag data obtained in the smooth condition, for which both the semispan and the full-span model were equipped with open flaps, showed good agreement. Drag data are presented in figure 7 for the semispan model in the smooth condition with both the solid and the open flap. The data with the open flap show drag coefficients lower than those for the solid flap by an amount approximately equal to the discrepancy between the semispan data and the full-span data in the rough condition.

For the plain wing in the rough condition, a difference exists between the pitching moments obtained in the two tests in the low to moderate range of lift coefficients (fig. 4(c)). At these lift coefficients, the pitching moments obtained in the semispan tests are more negative than those measured in the full-span tests by about 0.007. The reason for this discrepancy is not clear since it occurs only in this one case. Good agreement is shown in the pitching moments at these low lift coefficients for all the other conditions tested (figs. 3(c), 5(c), and 6(c)).

In only one case does there appear to be an important difference between the semispan and the full-span data. At a Reynolds number of 3.0×10^6 with both leading-edge and split flaps deflected, the pitching moments obtained from the semispan tests break in an unstable direction near maximum lift, whereas the pitching moments obtained from the full-span tests break in a stable direction just as they do at higher Reynolds numbers (fig. 6(c)). The addition of a fuselage to the full-span wing in a midwing or a high wing position (reference 7), however, changed the pitching-moment variation of the full-span arrangement near maximum lift at a Reynolds number of 6.8×10^6 so that it resembled the pitching-moment variation observed for the semi-span wing at a Reynolds number of 3.0×10^6 . It appears therefore that the effect of the tunnel-wall boundary layer on the measured characteristics of a semispan wing is similar in character but not as marked as the effect of adding a fuselage to the full-span wing in either a midwing or a high-wing position.

In order to establish the fact that these effects are caused by the tunnel-wall boundary layer rather than some other phenomena, tests were made in the Langley 19-foot pressure tunnel of the full-span wing with a center plate installed. The center plate extended approximately 1 chord length ahead of the leading edge and was fitted with a strip of screen wire which extended about 1/2 inch out from the plate to produce a boundary layer at the model which would simulate the tunnel-wall boundary layer in the Langley two-dimensional low-turbulence tunnel. The pitching-moment data with and without the center plate are shown in figure 8 and indicate results similar to those caused by the tunnel-wall boundary layer.

The conclusion reached from these results is that the effect of the boundary-layer flow over the root section is such as to delay the stall of this portion of the wing. Introduction of the boundary layer causes a high degree of turbulence in this region and, therefore, increases the effective Reynolds number of the root section. The scale effects on the maximum lift coefficient of this wing in the Reynolds number range from 3×10^6 to 6×10^6 are in the proper direction to produce this effect although they are not large. It is obvious, however, that the lift distribution on this configuration is such that both root and tip sections reach their maximum lift coefficients at very nearly the same angle of attack. Any effect tending to increase the maximum lift coefficient of the root would therefore cause the tip to stall first. Once the tip stalls, the loading on the root is decreased, which decreases its tendency to stall. A definite change in stability at the stall can be caused, therefore, by an effect which tends to delay even slightly the stall at the root. This investigation indicates that data obtained from semispan-wing tests in the Langley two-dimensional low-turbulence tunnel may be expected to be in good agreement with data obtained from

full-span tests of the wing alone except for unusually sensitive configurations where the lift distribution is such that small disturbances may cause a radical change in the location of the original stall or in the manner in which the stall progresses.

Data are presented in figure 9 which show the effect of leading-edge roughness at several Reynolds numbers on the aerodynamic characteristics of the wing with the leading-edge flap deflected both with and without the trailing-edge split flap. These data show that, in this configuration, the effect of leading-edge roughness is that the pitching-moment variation at the stall changes from stable to unstable. Pitching-moment data from full-span tests in the Langley 19-foot pressure tunnel with leading-edge roughness are shown in figure 10 and indicate a similar effect of roughness. This agreement between the full-span and the semispan data in the rough condition could be expected since the scale effects on wing sections with transition fixed at the leading edge are usually negligible.

Since experience has shown that manufacturing irregularities usually cause the aerodynamic characteristics of airplane wings to be similar to wind-tunnel data for similar configurations with some degree of roughness, it is recommended that the longitudinal stability characteristics measured with leading-edge roughness should be considered applicable to actual airplane designs.

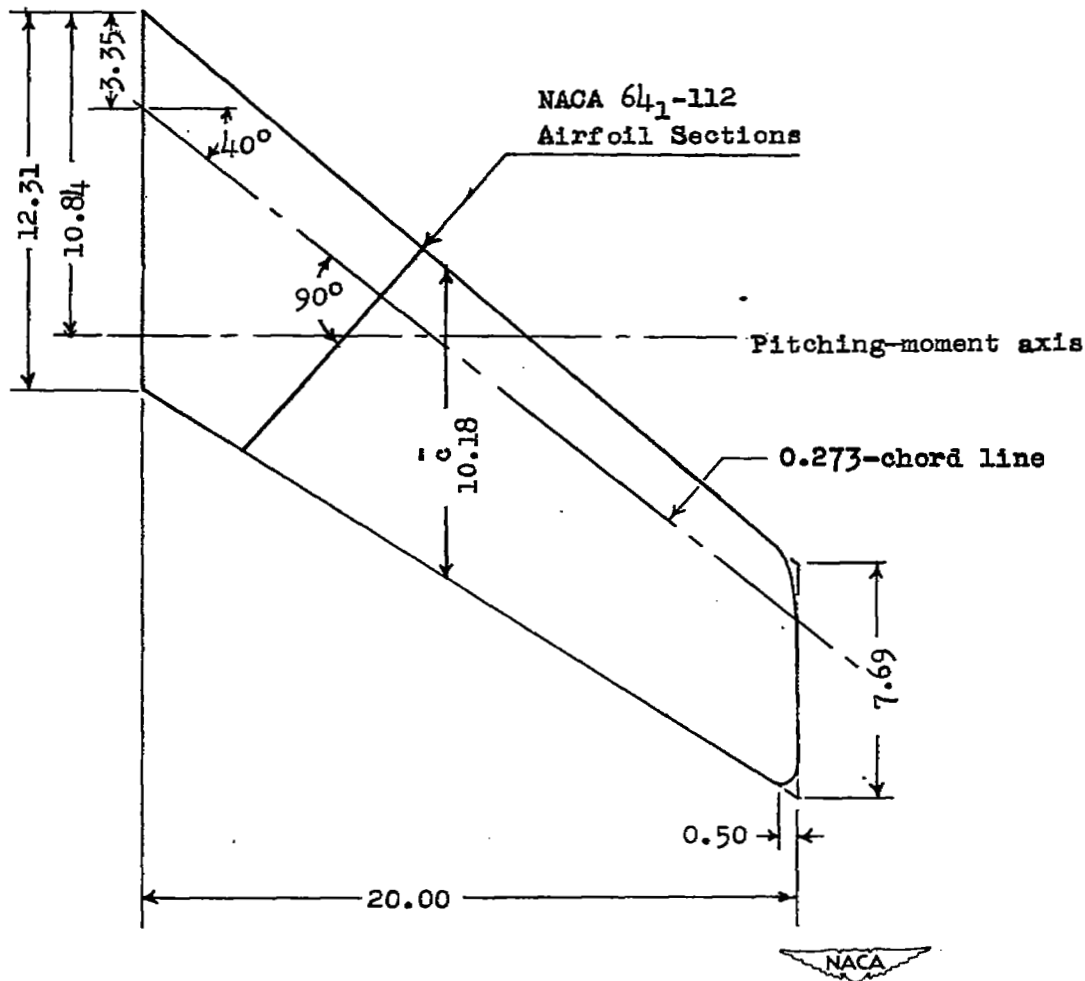
CONCLUDING REMARKS

This investigation indicates that data obtained from semispan wing tests in the Langley two-dimensional low-turbulence tunnel may be expected to be in good agreement with data obtained from full-span tests of the wing alone except for unusually sensitive configurations where the lift distribution is such that small disturbances may cause a radical change in the location of the original stall or in the manner in which the stall progresses. Data obtained for the wing with leading-edge roughness with both leading-edge and split flaps deflected indicate that the effect of leading-edge roughness is that the pitching-moment variation near maximum lift changes from stable to unstable. With roughness added, the full-span and semispan test results were in good agreement in all cases. Thus, it appears that adding roughness minimizes the influence of the tunnel-wall boundary layer.

Langley Aeronautical Laboratory
National Advisory Committee for Aeronautics
Langley Air Force Base, Va.

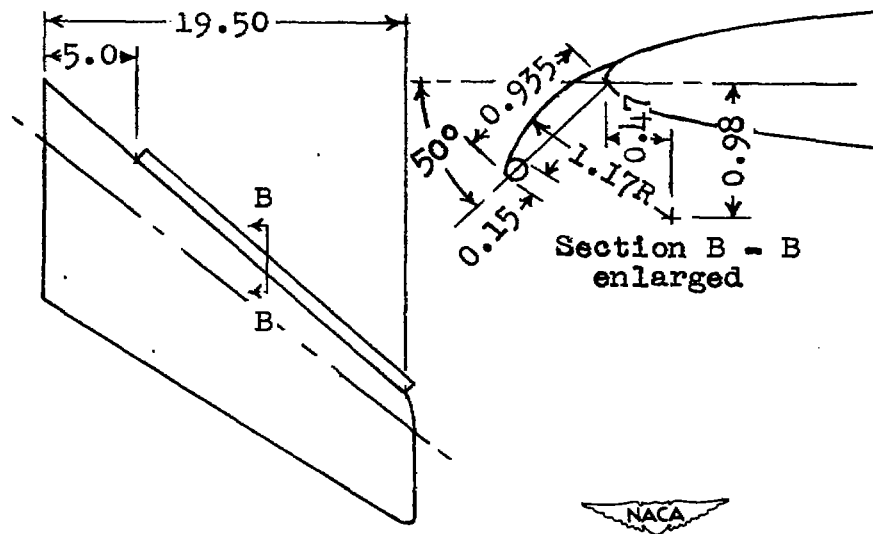
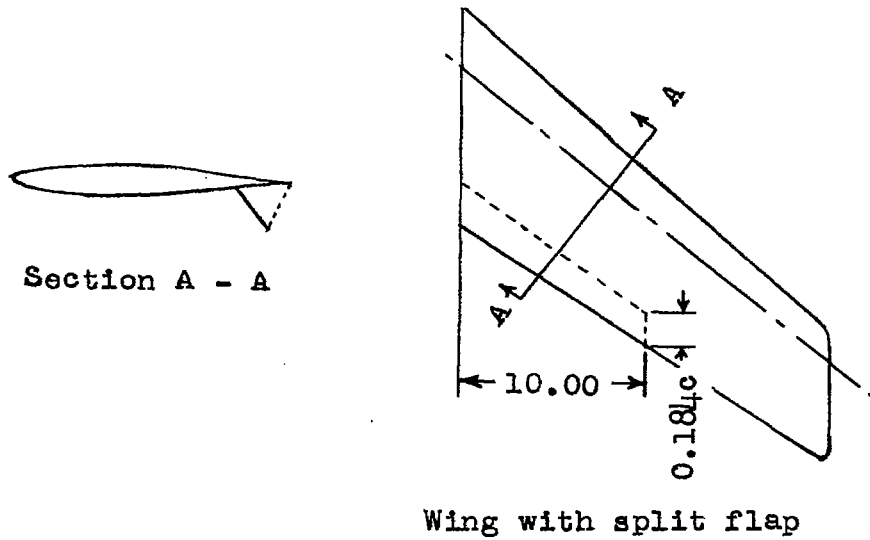
REFERENCES

1. Wilson, Herbert A., Jr., and Lovell, J. Calvin: Full-Scale Investigation of the Maximum Lift and Flow Characteristics of an Airplane Having Approximately Triangular Plan Form. NACA RM No. L6K20, 1946.
- 2. Neely, Robert H., and Conner, D. William: Aerodynamic Characteristics of a 42° Swept-Back Wing with Aspect Ratio 4 and NACA 64₁-112 Airfoil Sections at Reynolds Numbers from 1,700,000 to 9,500,000. NACA RM No. L7D14, 1947.
3. Von Doenhoff, Albert E., and Abbott, Frank T., Jr.: The Langley Two-Dimensional Low-Turbulence Pressure Tunnel. NACA TN No. 1283, 1947.
4. Conner, D. William, and Neely, Robert H.: Effects of a Fuselage and Various High-Lift and Stall-Control Flaps on Aerodynamic Characteristics in Pitch of an NACA 64-Series 40° Swept-Back Wing. NACA RM No. L6L27, 1947.
5. Katzoff, S., and Hannah, Margery E.: Calculation of Tunnel-Induced Upwash Velocities for Swept and Yawed Wings. NACA TN No. 1748, 1948.
- 6. Furlong, G. Chester, and Bollech, Thomas V.: Effect of Ground Interference on the Aerodynamic Characteristics of a 42° Swept-back Wing. NACA RM No. L8F04, 1948.
- 7. Graham, Robert R., and Conner, D. William: Investigation of High-Lift and Stall-Control Devices on an NACA 64-Series 42° Sweptback Wing with and without Fuselage. NACA RM No. L7G09, 1947.



(a) Wing plan form.

Figure 1.- Details of semispan sweptback wing model. Aspect ratio = 4.01; semispan area = 199.8 sq. in. (All dimensions in inches).



(b) Details of various devices on wing.
Figure 1.- Concluded.

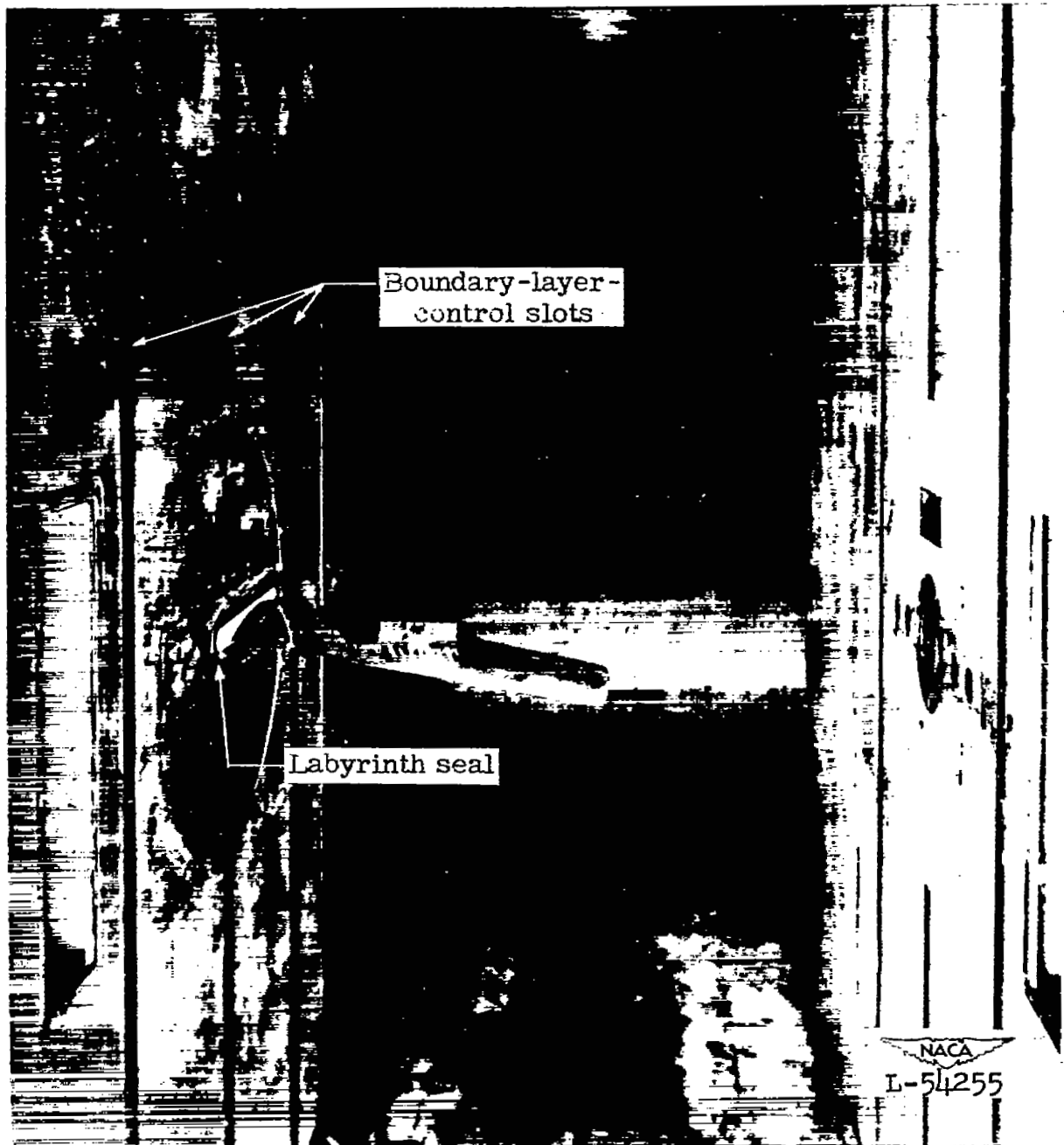
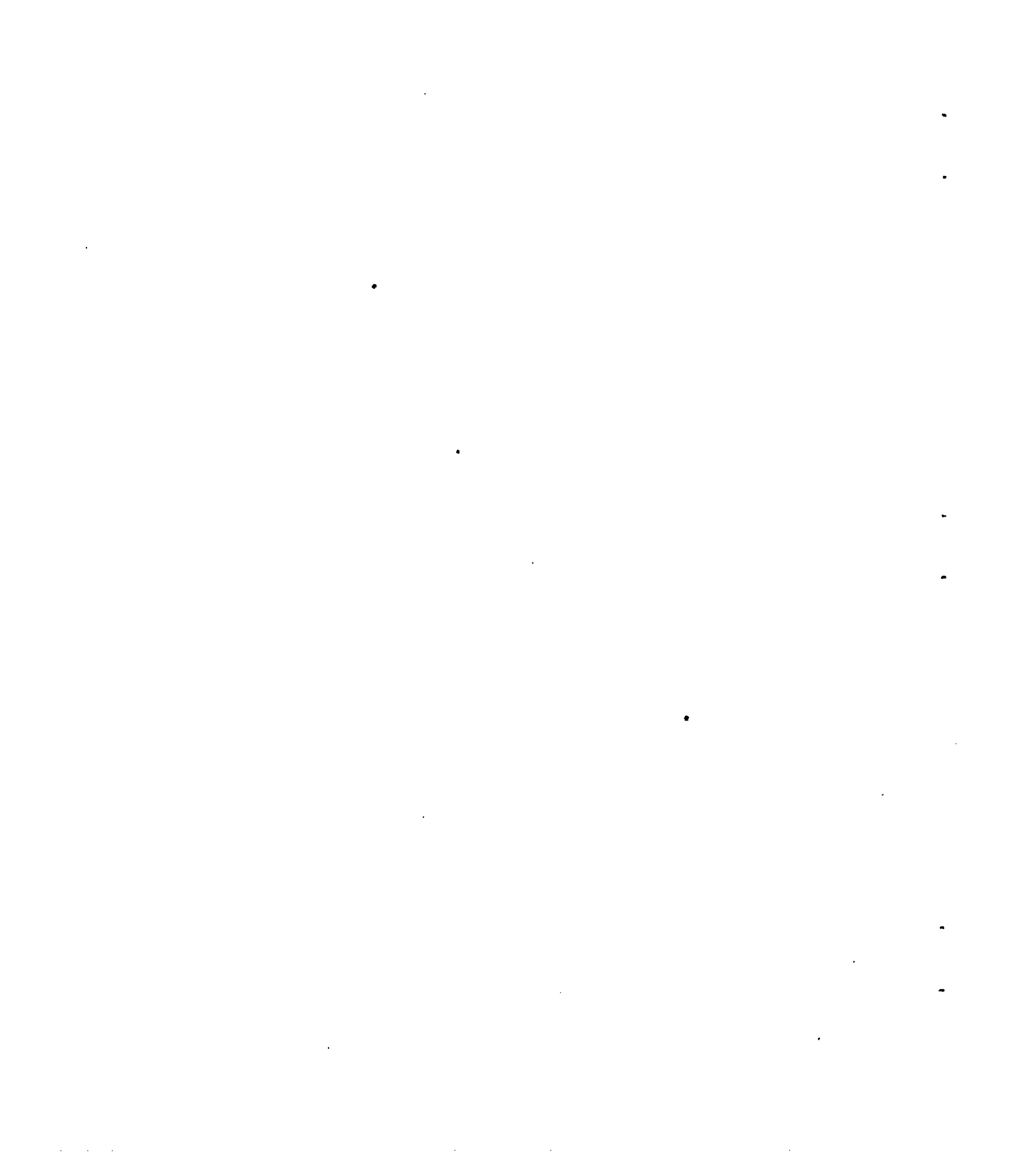
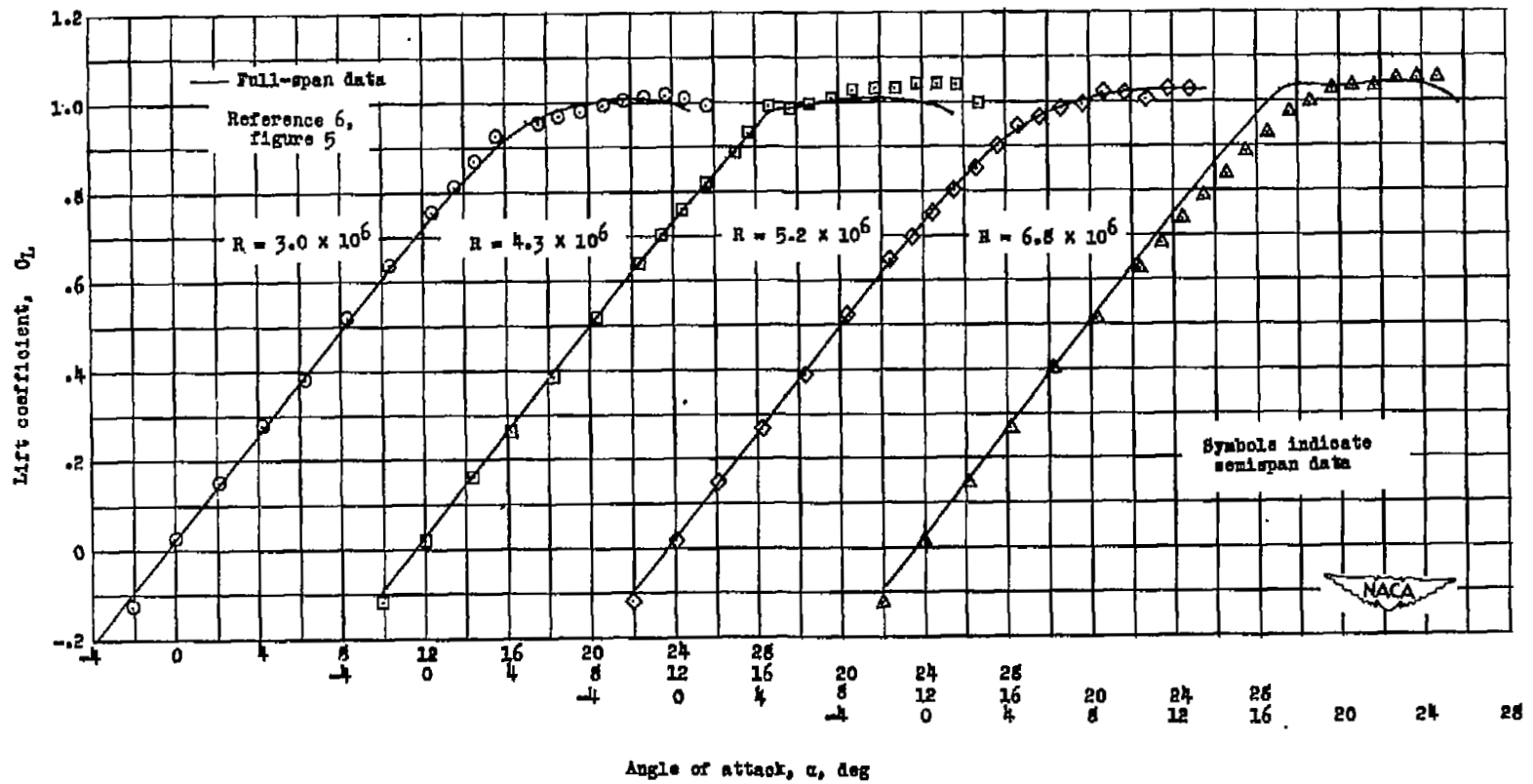


Figure 2.- Rear view of 40° sweptback wing model installed in Langley two-dimensional low-turbulence pressure tunnel.





(a) Lift.

Figure 3.- Comparison between data on a full-span model and a semispan model of a 40° sweptback wing.

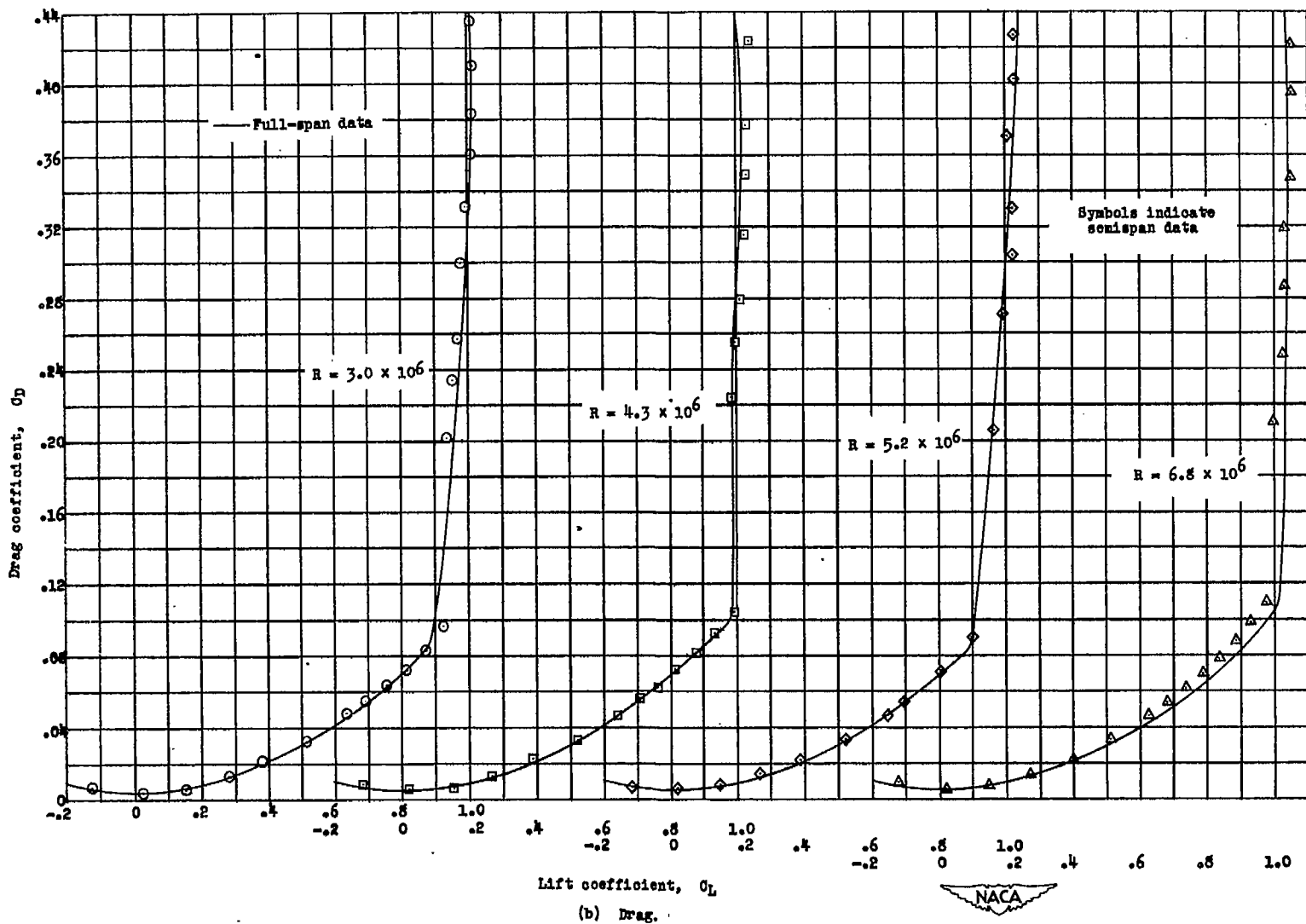
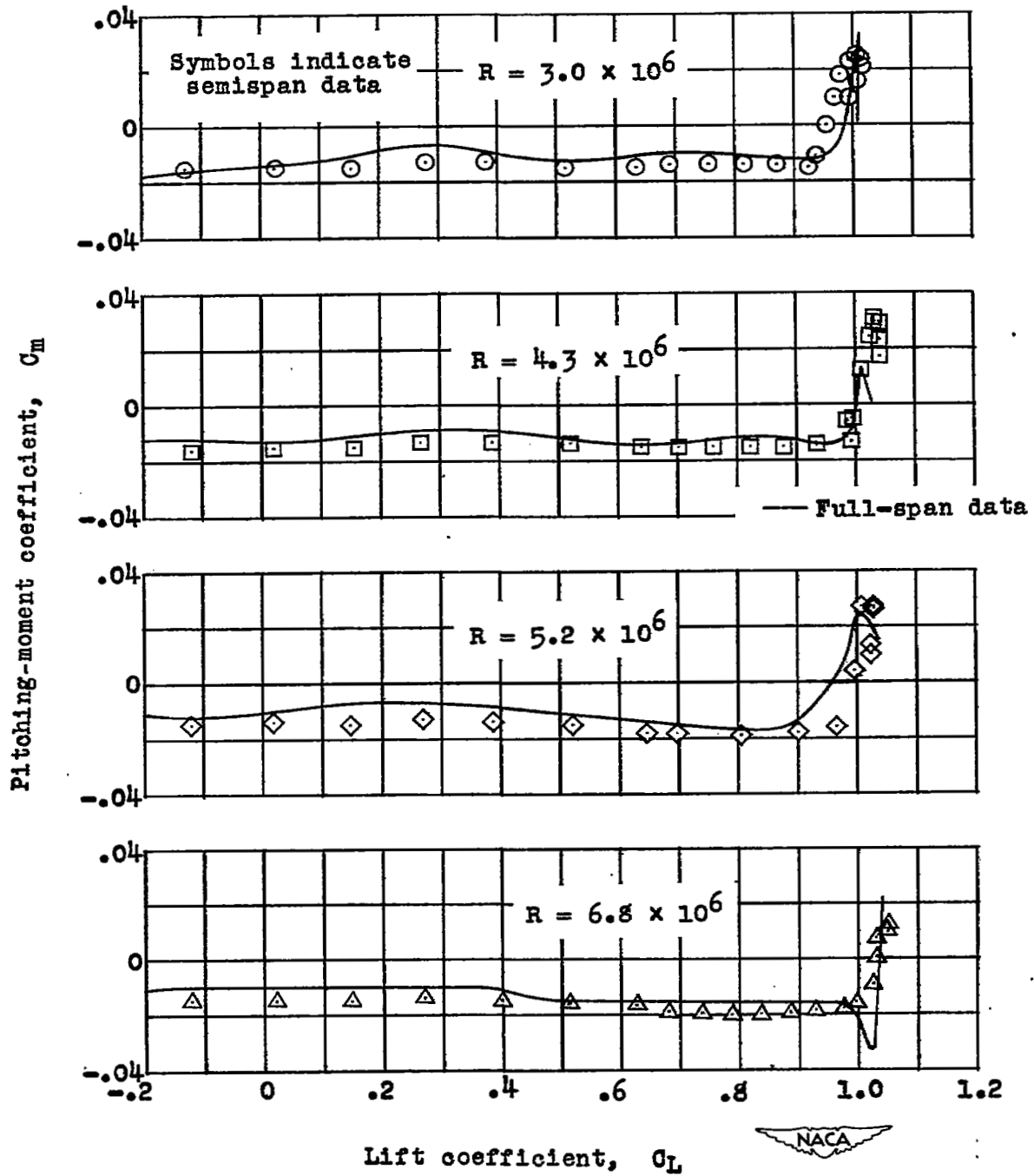
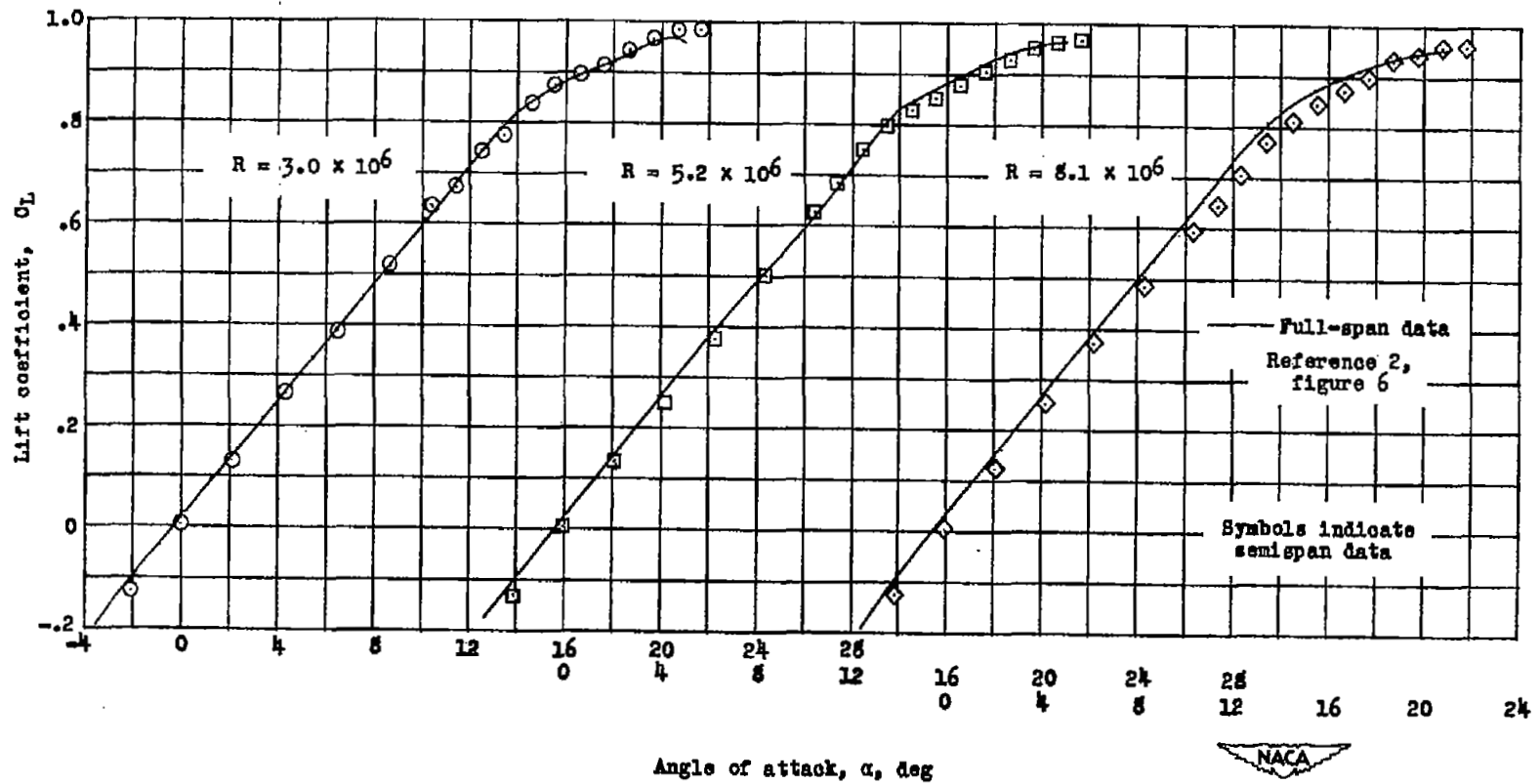


Figure 3.- Continued.



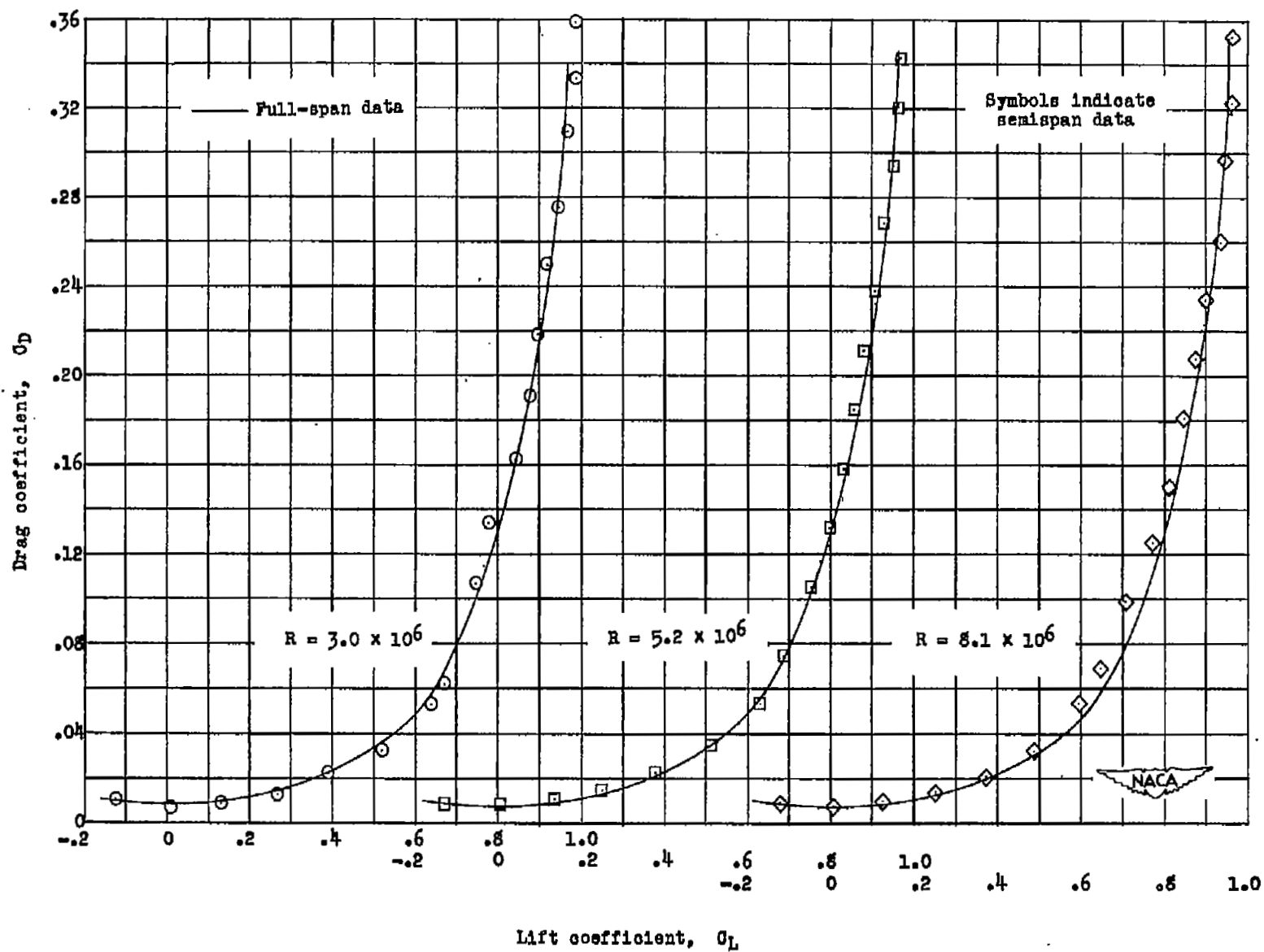
(c) Pitching moment.

Figure 3.- Concluded.



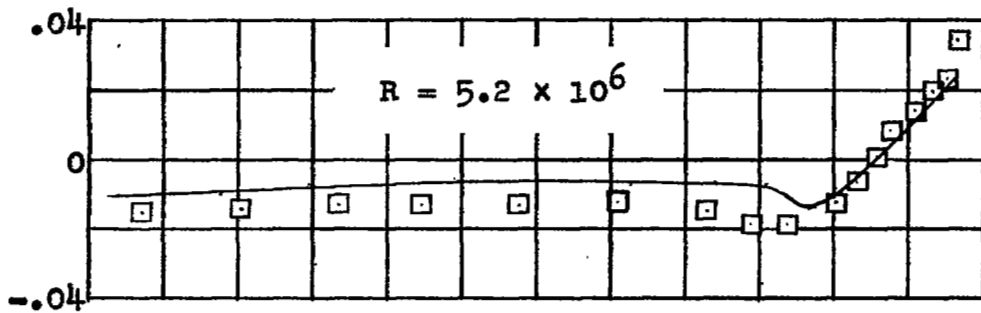
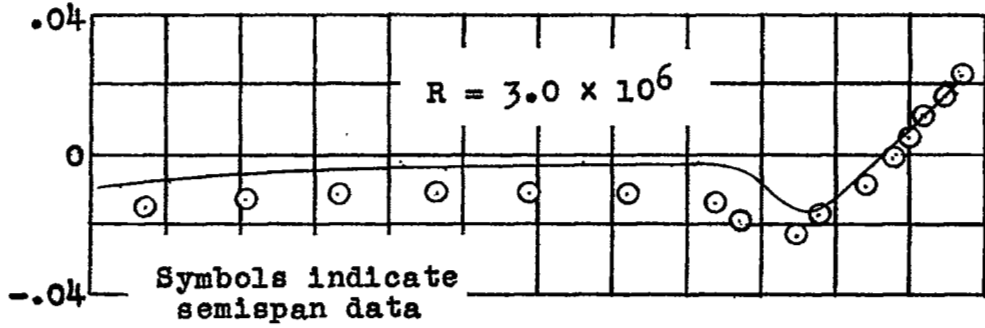
(a) Lift.

Figure 4.- Comparison between data on a full-span model and a semispan model of a 40° sweptback wing with leading-edge roughness.

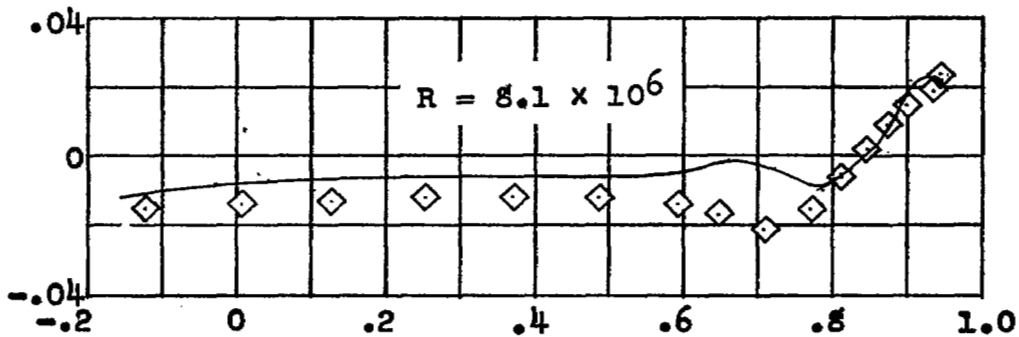


(b) Drag.

Figure 4.- Continued.



— Full-span data

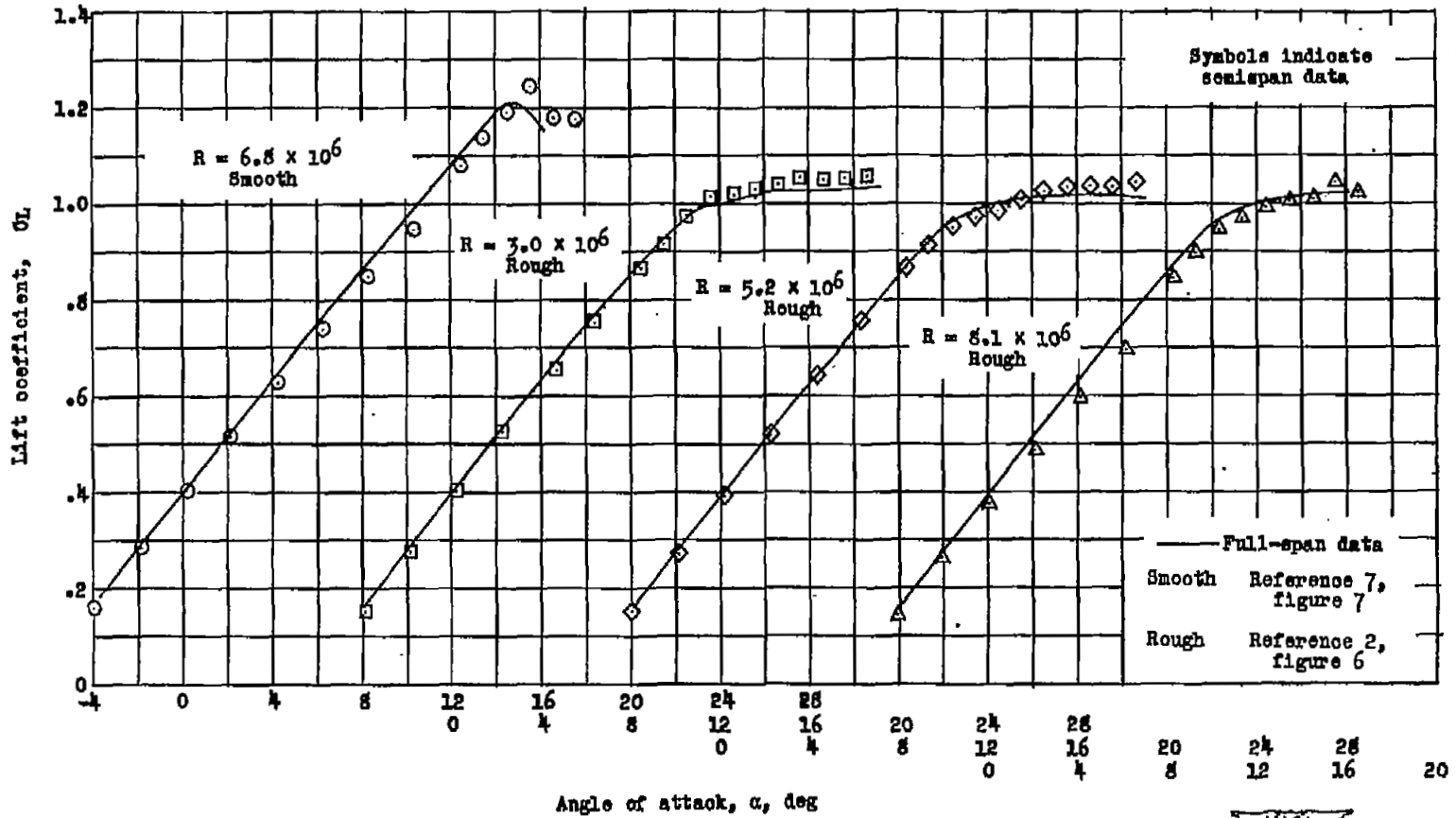


Lift coefficient, C_L



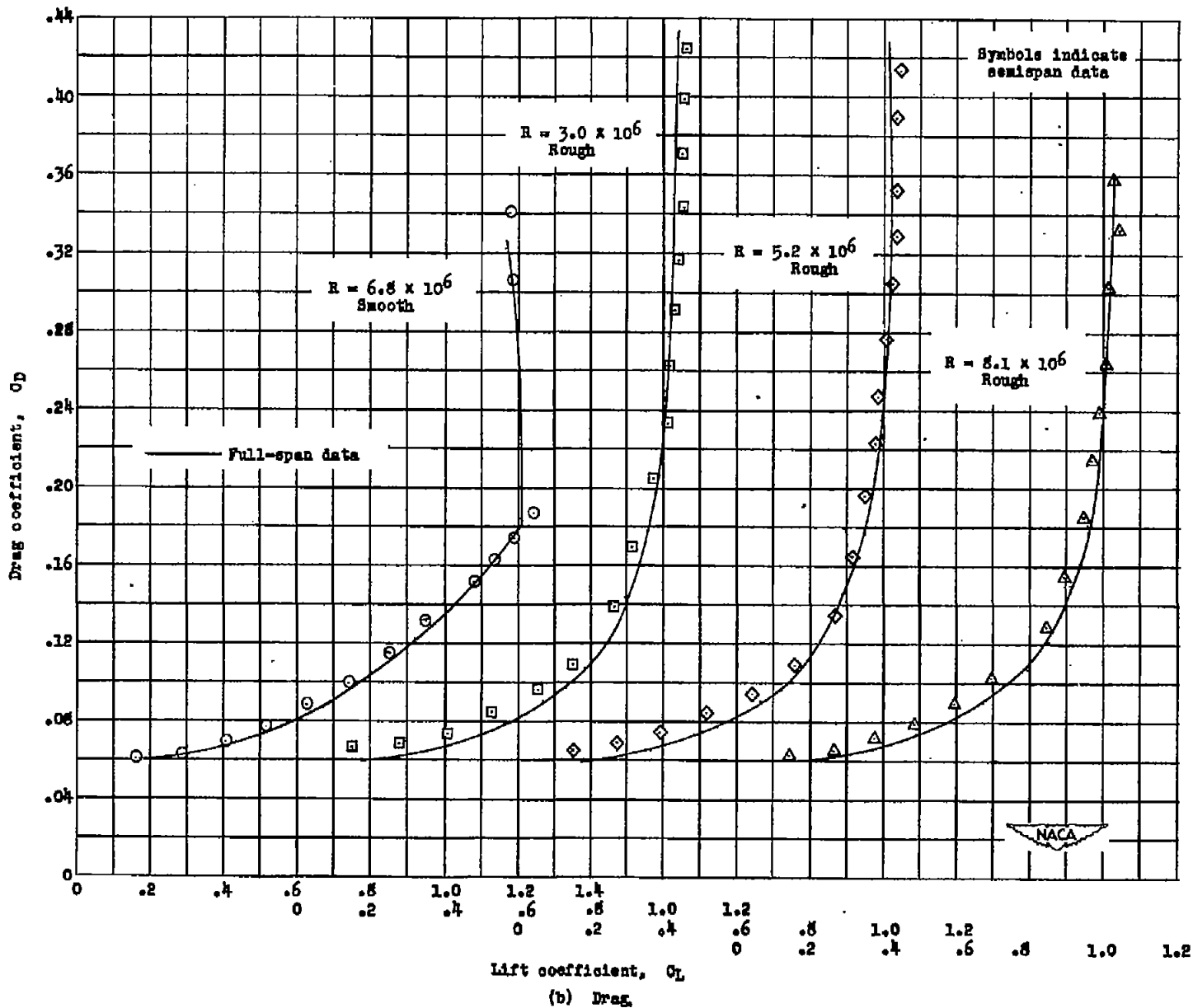
(c) Pitching moment.

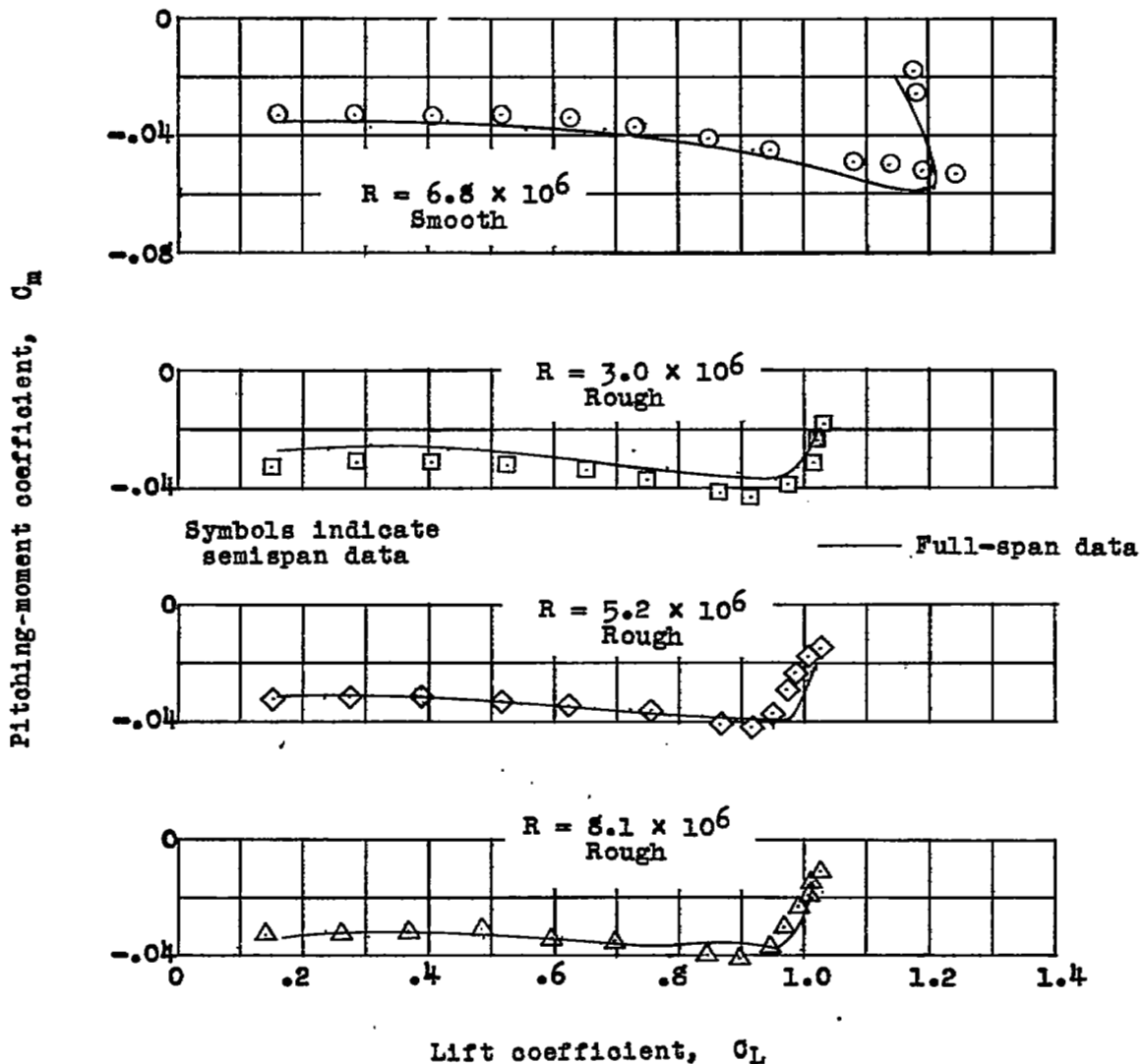
Figure 4.- Concluded.



(a) Lift.

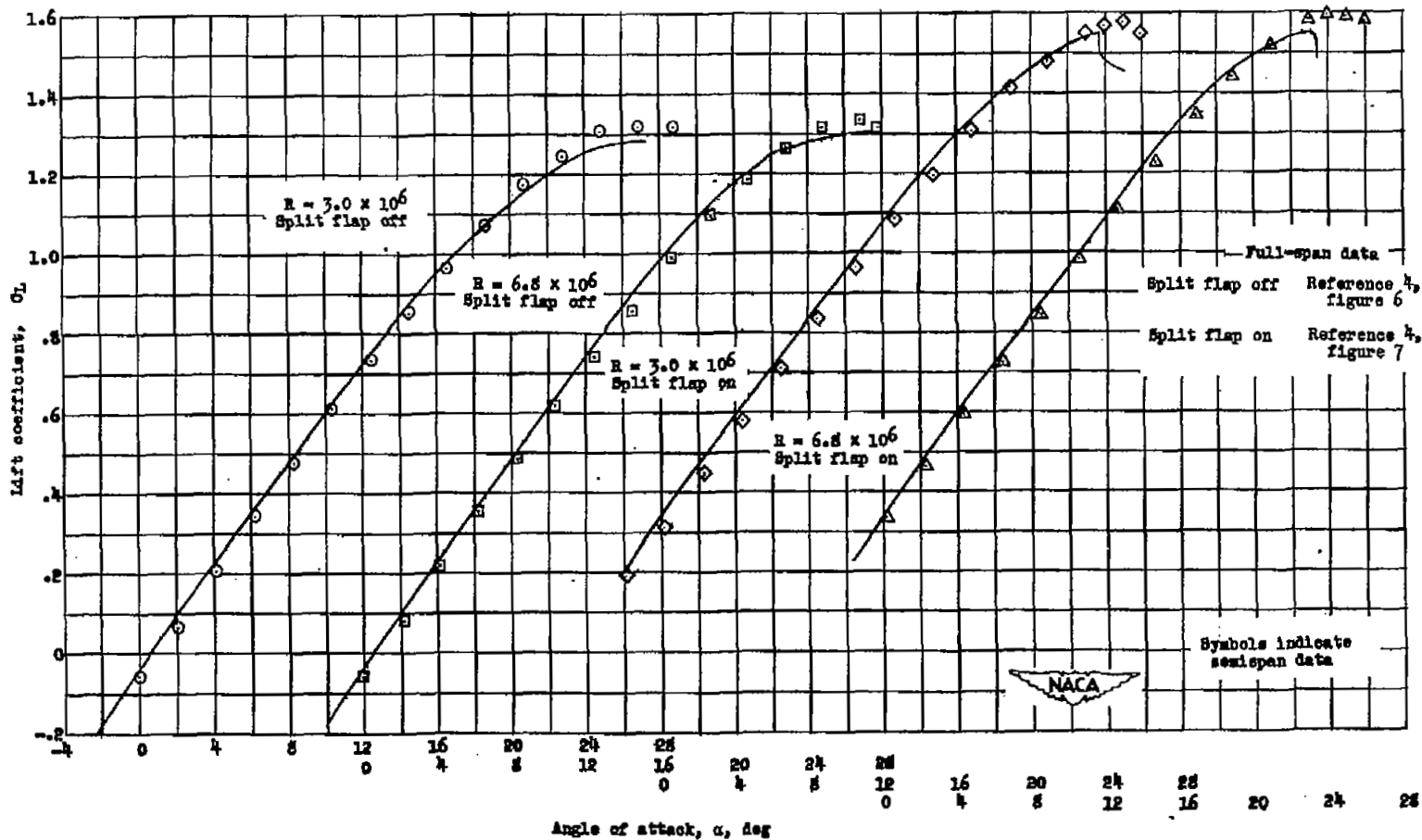
Figure 5.- Comparison between data on a full-span model and a semispan model of a 40° sweptback wing equipped with 0.5 $b/2$ split flaps.





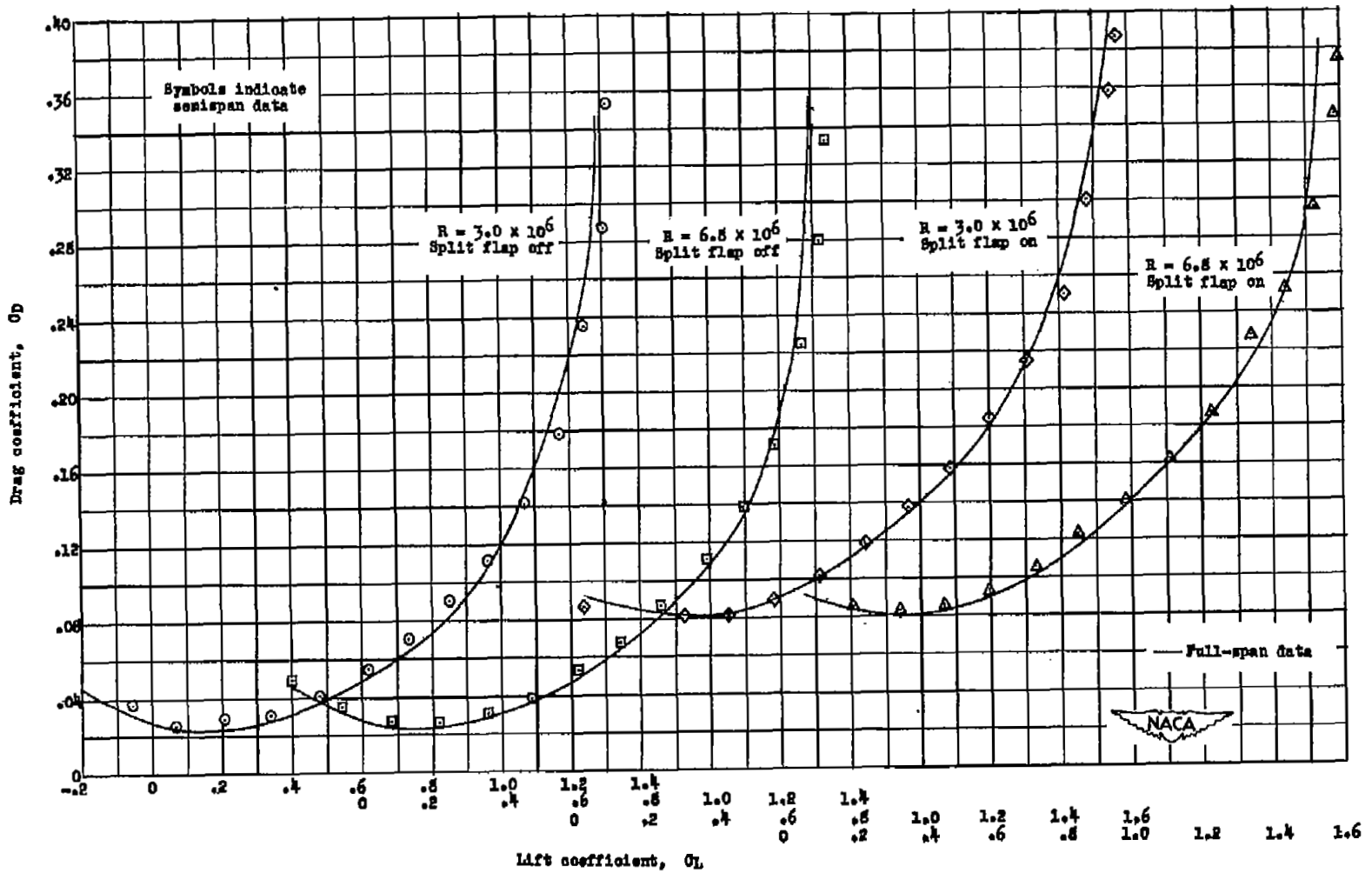
(c) Pitching moment.

Figure 5.- Concluded.



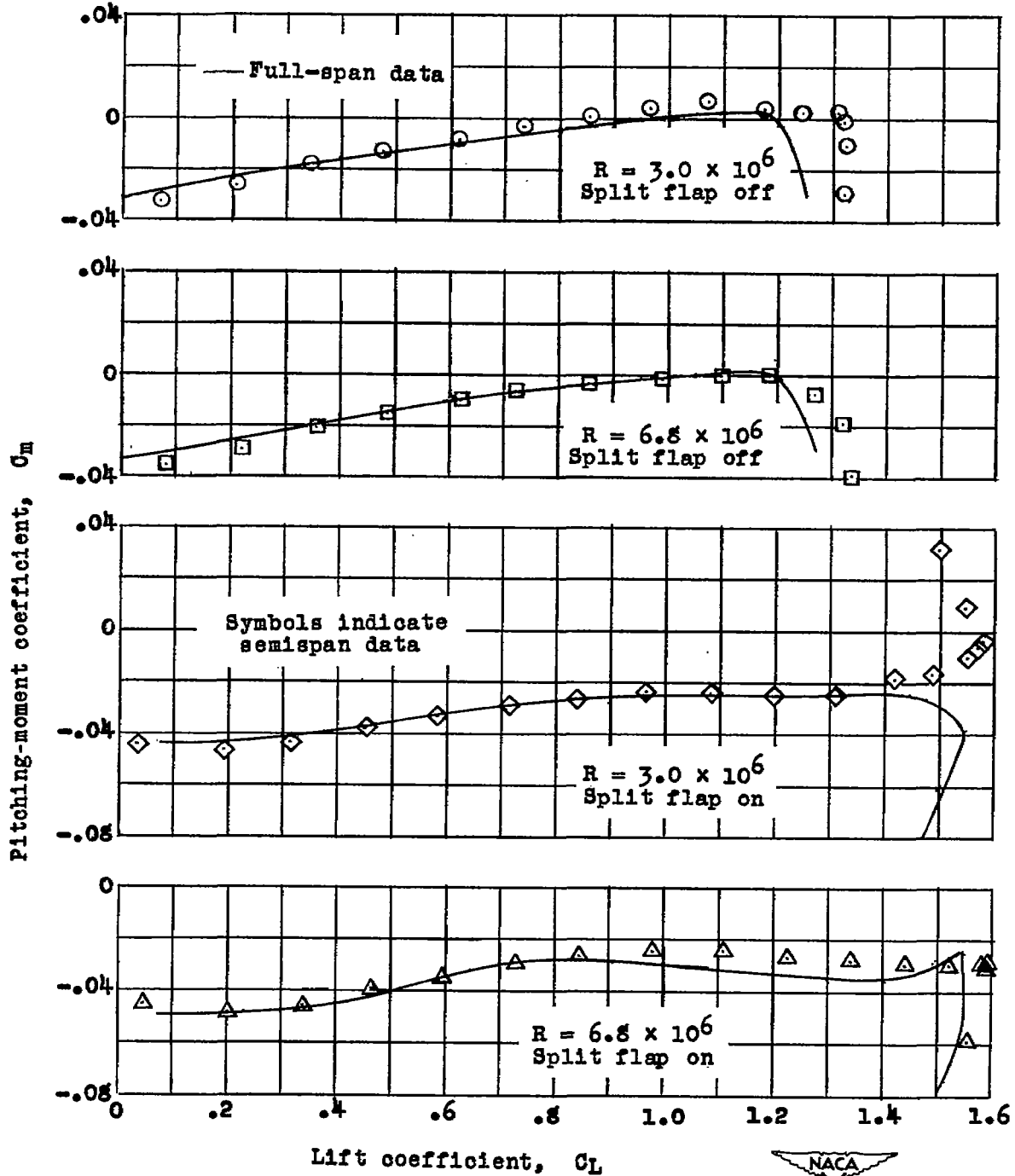
(a) Lift.

Figure 6.- Comparison between data on a full-span model and a semispan model of a 40° sweptback wing equipped with $0.725 b/2$ leading-edge flaps.



(b) Drag.

Figure 6.- Continued.



(c) Pitching moment.

Figure 6.- Concluded.

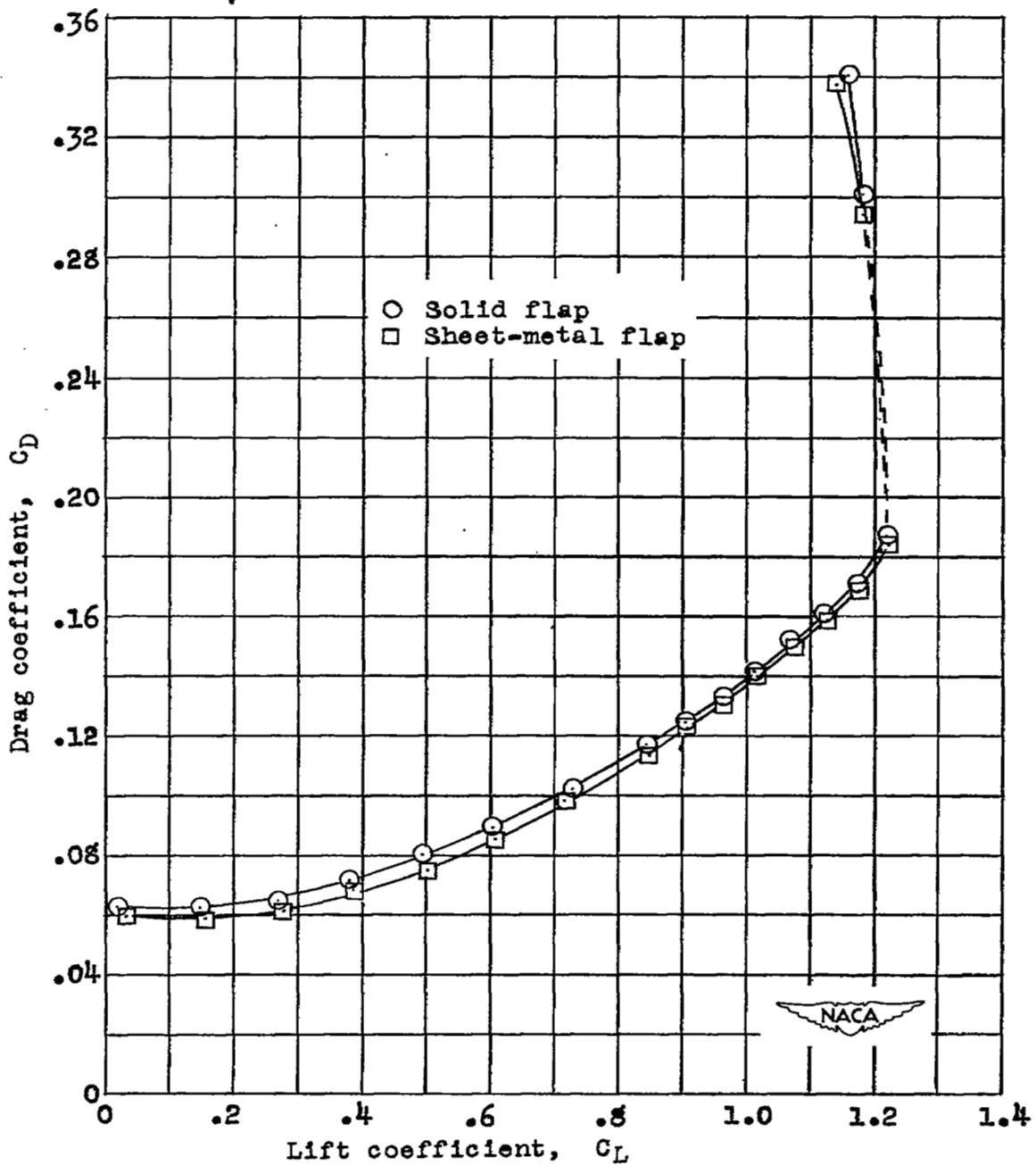


Figure 7.- Comparison between drag characteristics measured with a solid flap and with a bent sheet-metal flap.

$R = 8.1 \times 10^6$. Model smooth.

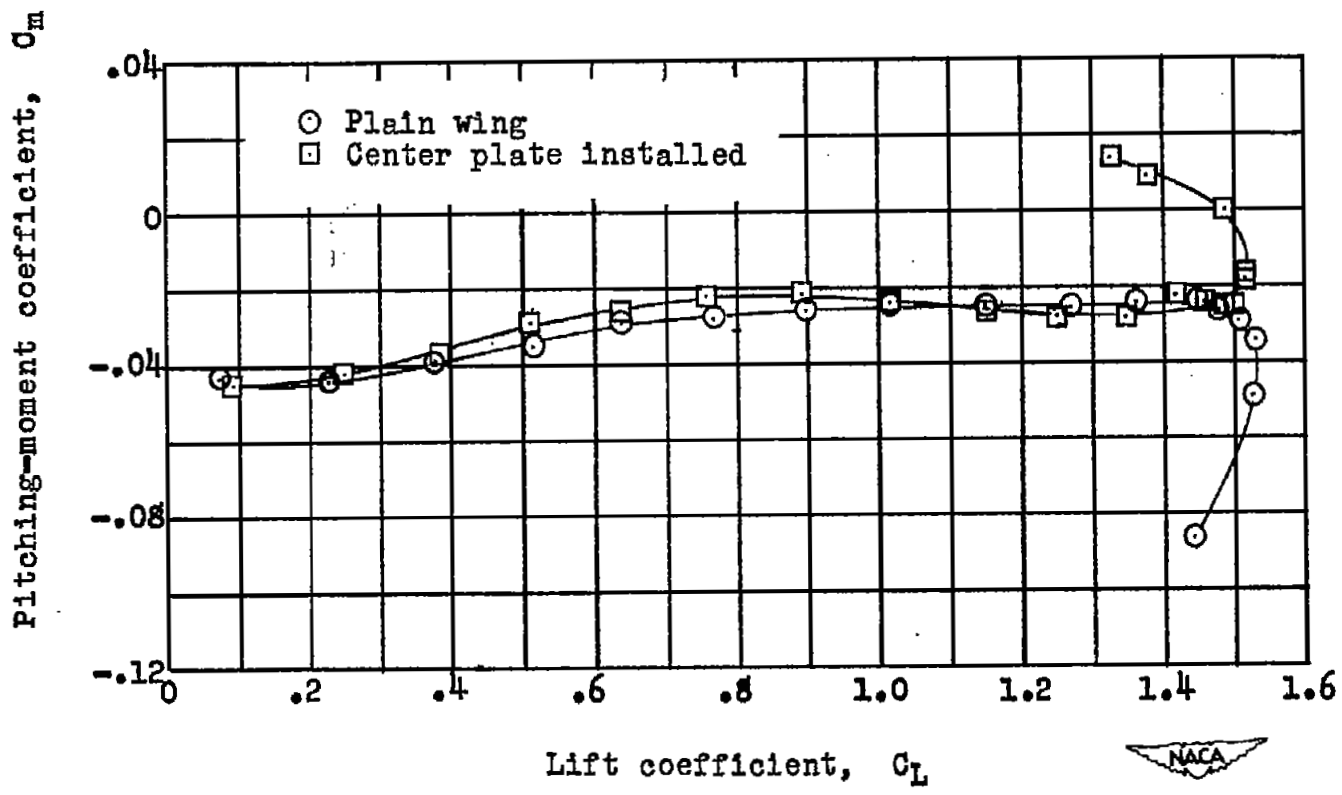
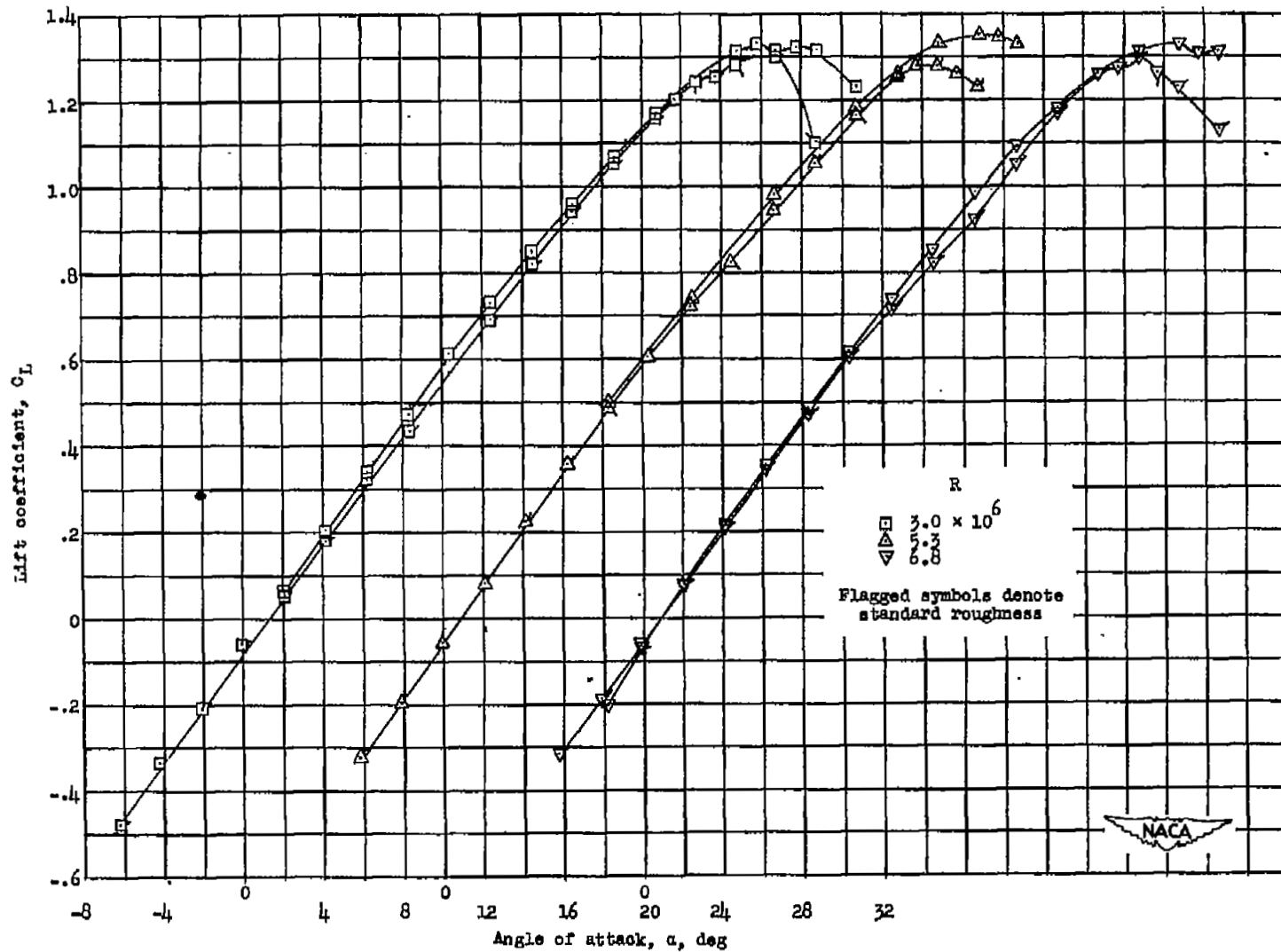


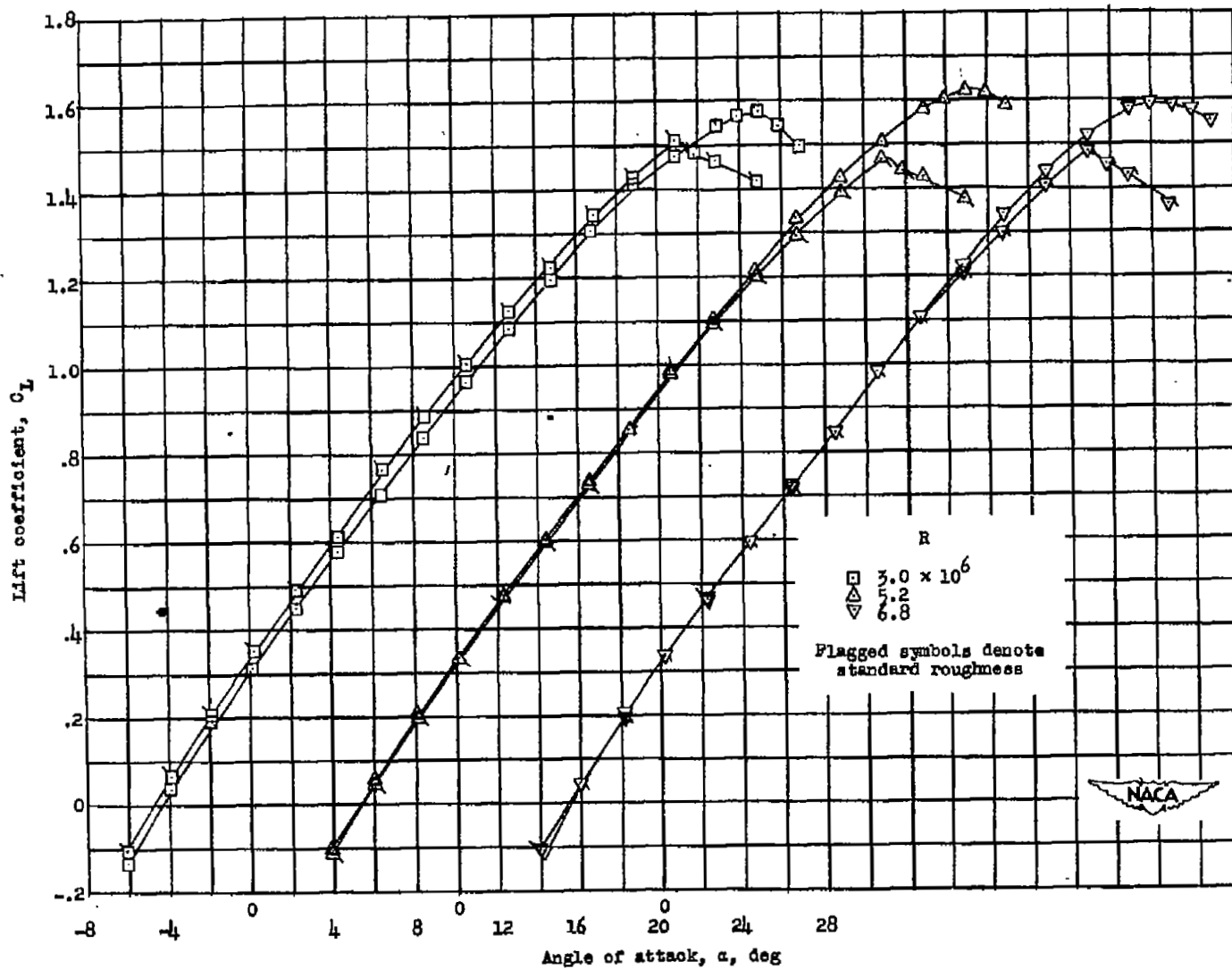
Figure 8.- Comparison of pitching-moment data obtained on a full-span model of a 40° sweptback wing with and without center plate. Leading-edge and split flaps deflected. $R = 3.0 \times 10^6$.



(a) Lift, split flap off.

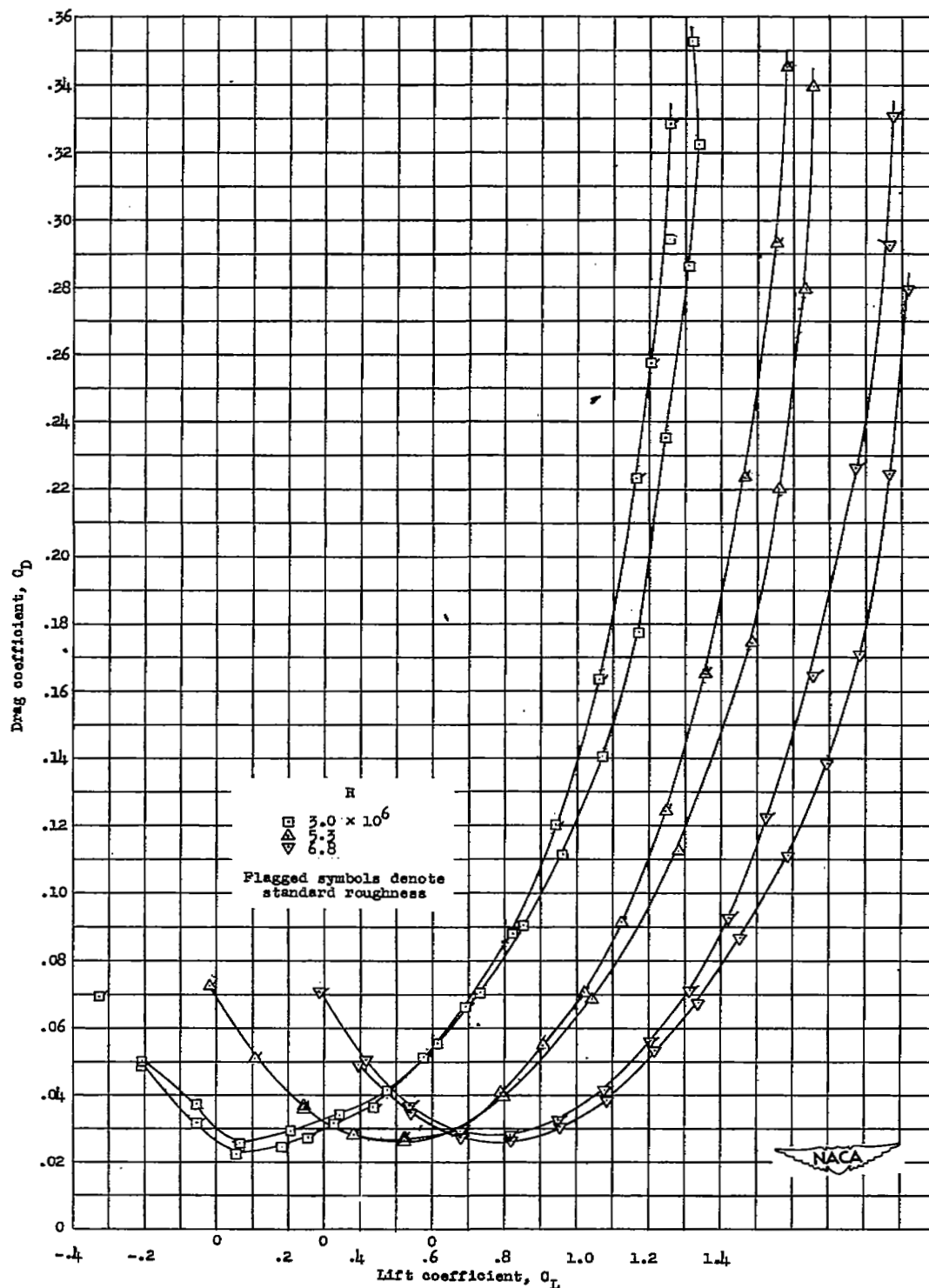
Figure 9.- Aerodynamic characteristics of a 40° sweptback wing equipped with a $0.725 b/2$ extensible leading-edge flap with and without roughness at various Reynolds numbers.

Semi-span Model



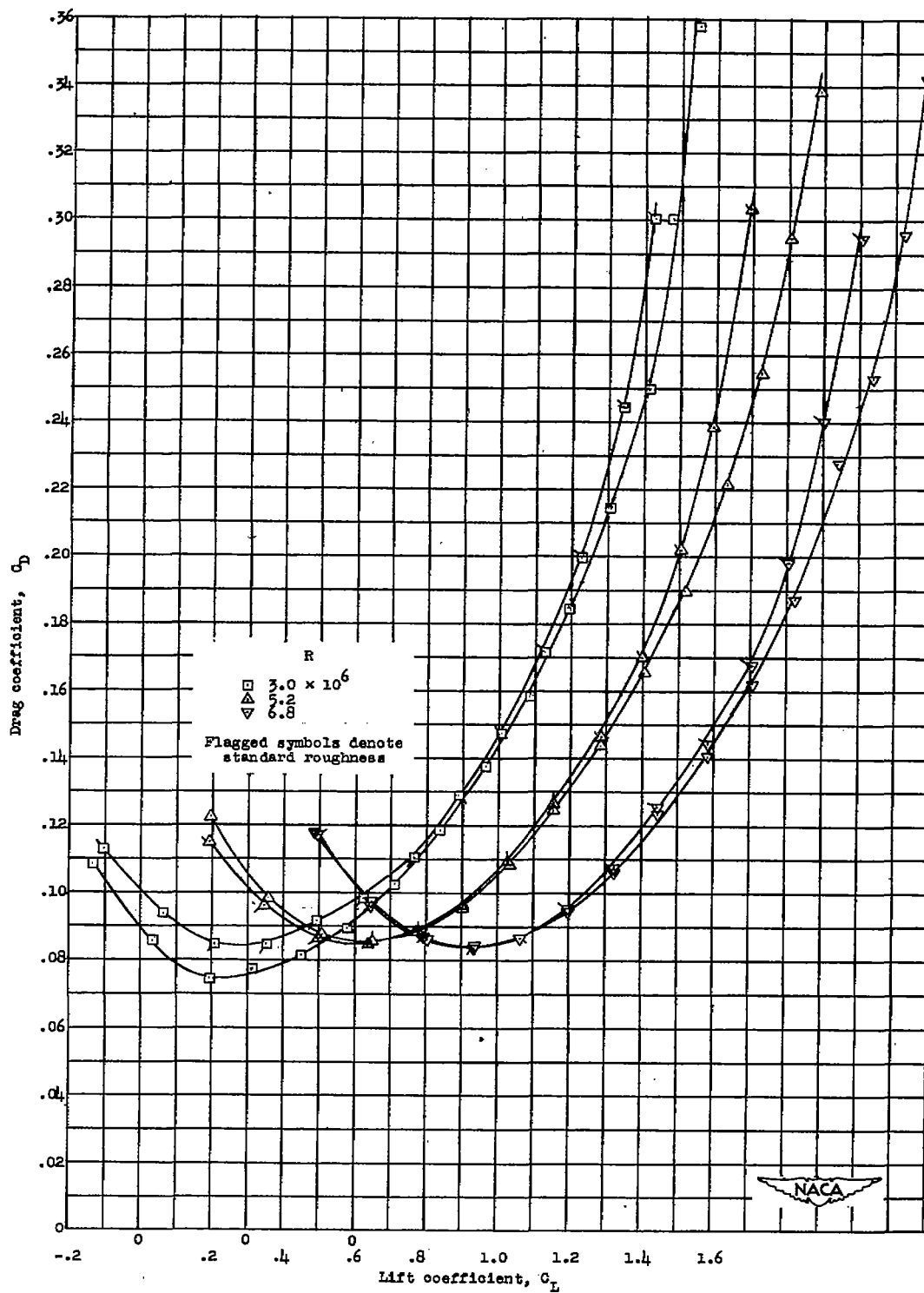
(b) Lift, split flap on.

Figure 9.- Continued.

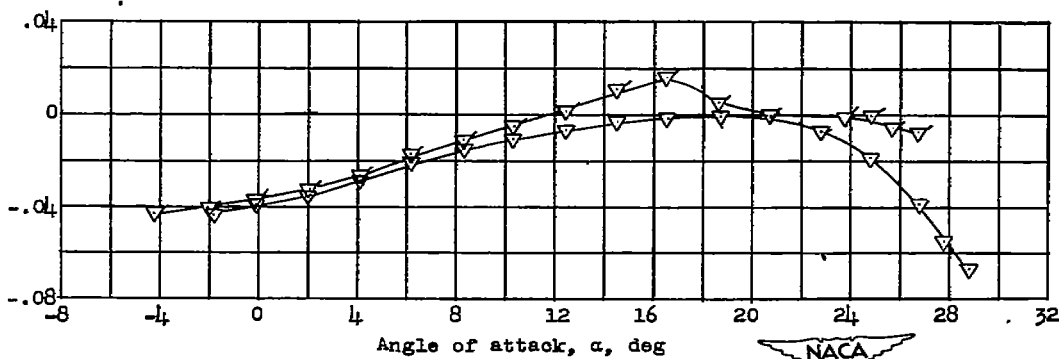
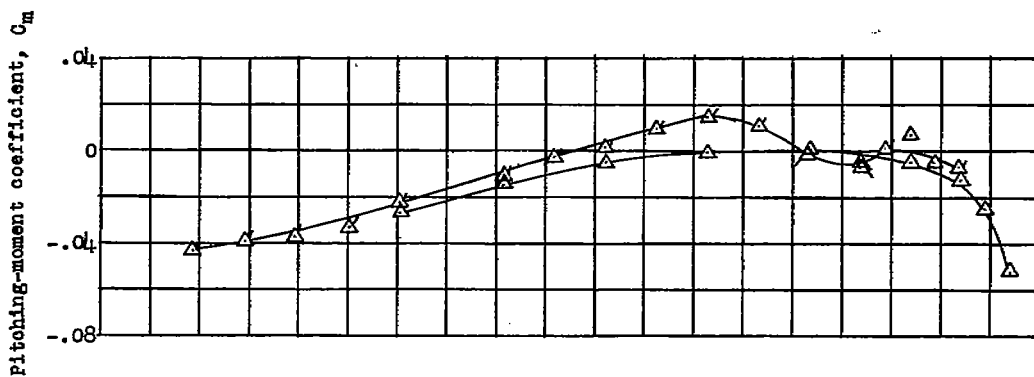
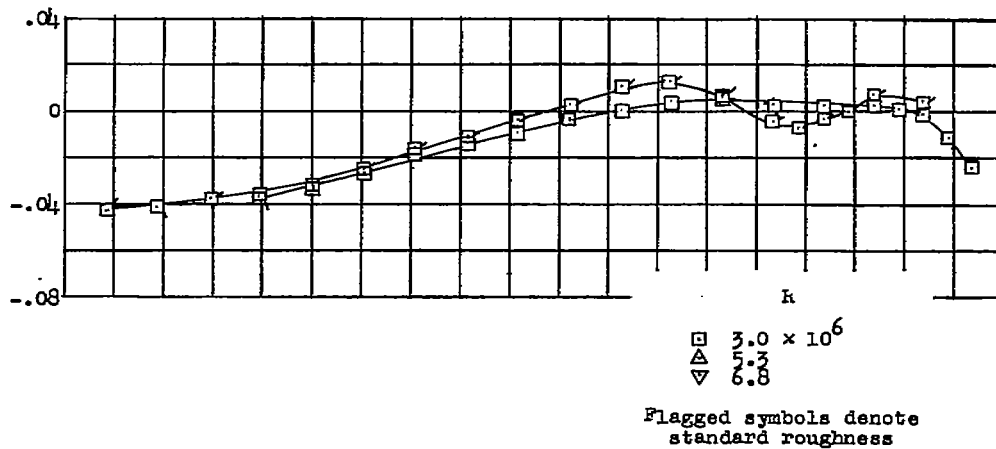


(c) Drag, split flap off.

Figure 9.- Continued.



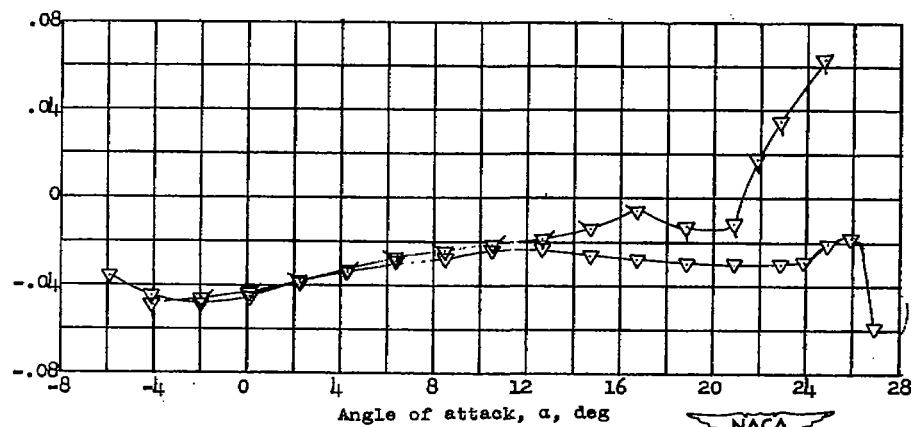
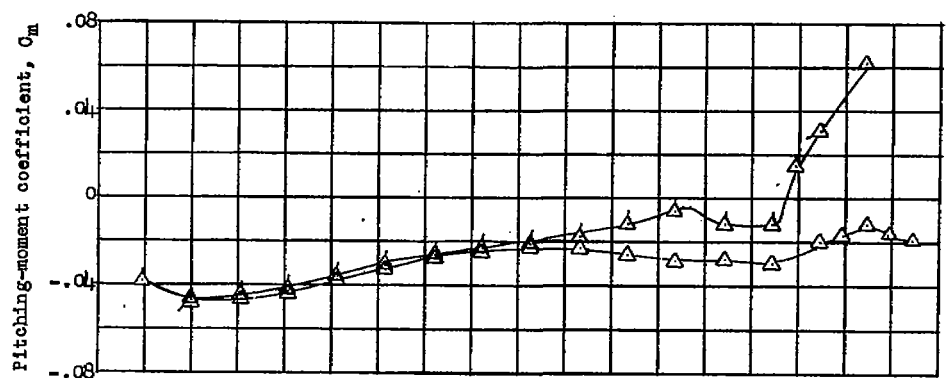
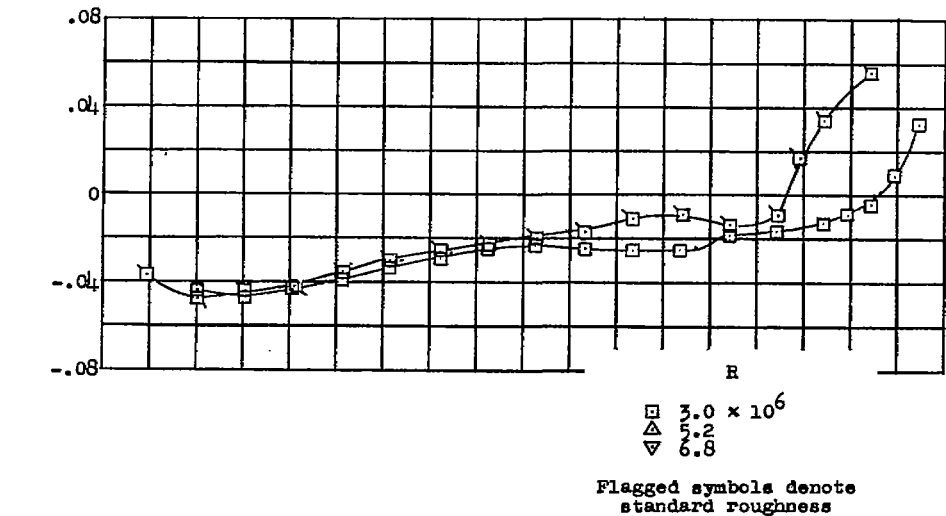
(d) Drag, split flap on.
 Figure 9.- Continued.



(e) Pitching moment, split flap off.

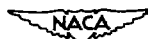
Figure 9.- Continued.





(f) Pitching moment, split flap on.

Figure 9.- Concluded.



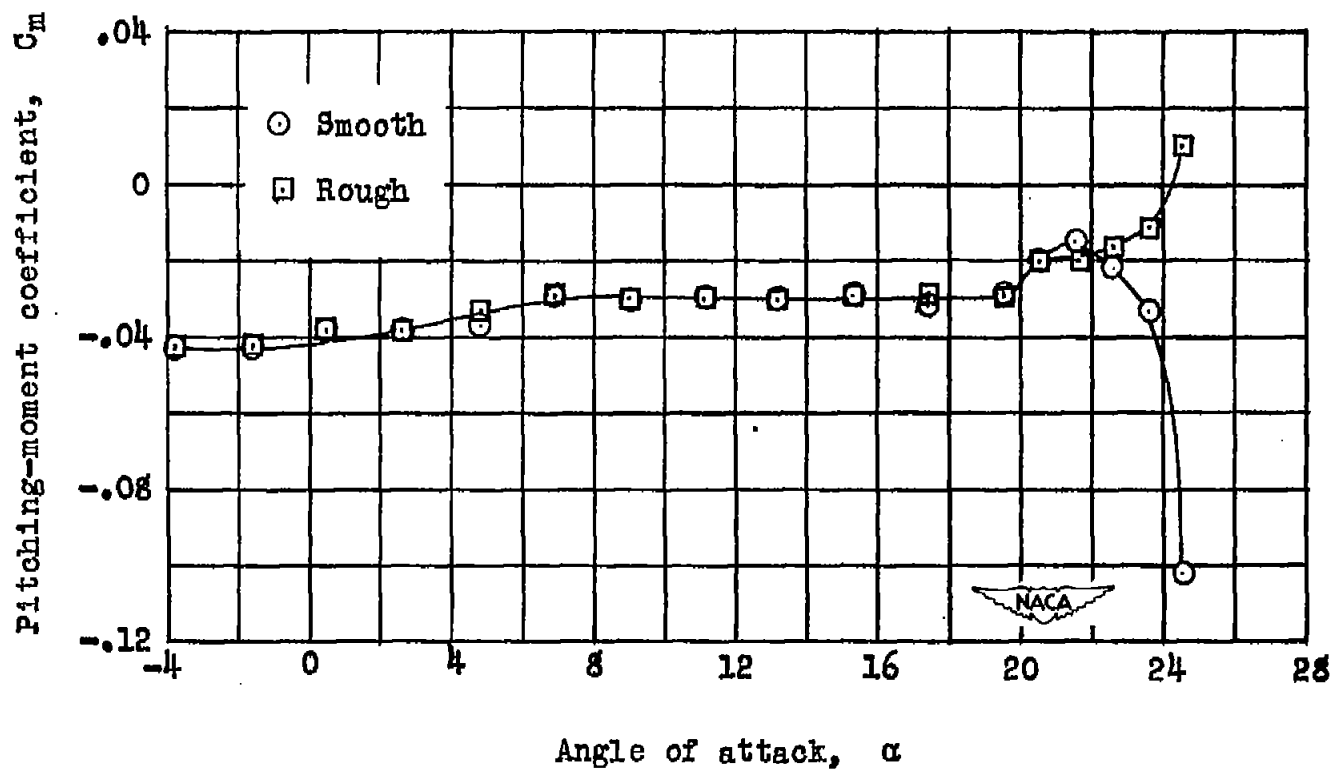


Figure 10.- Pitching-moment characteristics of a 40° sweptback wing with and without roughness from full-span tests in Langley 19-foot pressure tunnel. Leading-edge and split flap deflected. $R = 2.8 \times 10^6$.

NASA Technical Library



3 1176 01436 7222